

# Giant transmission and dissipation in perforated films mediated by surface phonon polaritons

D. Korobkin, Y. Urzhumov, B. Neuner III, and G. Shvets\*

*Department of Physics, The University of Texas at Austin, Austin, Texas 78712*

Z. Zhang and I. D. Mayergoyz

*Department of Electrical and Computer Engineering,*

*University of Maryland, College Park, MD 20742*

(Dated: August 12, 2018)

## Abstract

We experimentally and theoretically study electromagnetic properties of optically thin silicon carbide (SiC) membranes perforated by an array of sub-wavelength holes. Giant absorption and transmission is found using Fourier Transformed Infrared (FTIR) microscopy and explained by introducing a frequency-dependent effective permittivity  $\epsilon_{\text{eff}}(\omega)$  of the perforated film. The value of  $\epsilon_{\text{eff}}(\omega)$  is determined by the excitation of two distinct types of hole resonances: a delocalized slow surface polariton (SSP) whose frequency is largely determined by the array period, and a localized surface polariton (LSP) which corresponds to the resonances of an isolated hole. Only SSPs are shown to modify  $\epsilon_{\text{eff}}(\omega)$  strongly enough to cause giant transmission and absorption.

PACS numbers: 41.20.Cv, 42.70.Qs, 42.25.BS, 71.45.Gm

---

\*Electronic address: gena@physics.utexas.edu

Diffraction of light is the major obstacle to increasing the density of optical circuits and integrating them with electronics [1]: light cannot be confined to dimensions much smaller than half of its wavelength  $\lambda/2$ . Utilizing materials with a negative dielectric permittivity circumvents diffraction limit because interfaces between polaritonic ( $\epsilon < 0$ ) and dielectric ( $\epsilon > 0$ ) materials support quasi-electrostatic waves (surface polaritons) that can be confined to sub- $\lambda$  dimensions. Negative  $\epsilon$  can be due to either collective oscillation of conduction electron in metals (plasmons) [2] or lattice vibrations in polar crystals such as ZnSe, SiC, InP [3]. Both metallic and SiC interfaces have been shown to guide surface plasmon (and phonon) polaritons over long distances [4, 5, 6], support negative-index waves [7, 8, 9], and serve as elements of a super-lens [10, 11, 12]. Therefore, the explosion of research aims at understanding basic polaritonic components: grooves in metal films [13], nanoparticle-film polaritons [14], hole arrays [15], and single holes [16].

Sub- $\lambda$  hole arrays were the first to attract significant attention after the discovery of extraordinary optical transmission [15] through perforated optically thick metallic films and the ensuing controversy [17, 18] about the role of surface polaritons in transmission enhancement. The difficulty with interpreting the role of surface polaritons (SPs) in transmission through optically thick ( $\lambda_{\text{skin}} \equiv \lambda/4\pi\sqrt{|\epsilon|} \ll H$ , where  $H$  is the film thickness) films arises from the fact that even holes in a perfect conductor (which does not support surface polaritons) can spoof surface polaritons [19], especially when  $\lambda$  is close to array period  $L$ . No such spoofing occurs for optically thin films.

In this Letter we report results of the spectroscopic study of such suspended perforated SiC membranes, with both hole diameter  $D \ll \lambda$  and period  $L < \lambda$  significantly sub- $\lambda$ . SiC is chosen because of its low losses [3] and the possibility of growing high quality thin SiC films on Si substrates [20]. While the majority of surface phonon polariton experiments to-date have been conducted with SiC substrates [3, 6, 21], thin SiC membranes hold a greater promise for fabricating novel multi-layer nanophononic structures [12]. Using FTIR microscopy, we demonstrate that, in adjacent frequency ranges, giant transmission and absorption of the incident radiation is realized. Both phenomena are shown to be due to the excitation of quasi-electrostatic SPs. It is shown that a perforated film can be described as a metamaterial with the effective permittivity  $\epsilon_{\text{eff}} = \epsilon_r + i\epsilon_i$  strongly modified by the excitation of SPs: regions of giant transmission and absorption are related, respectively, to the lowering of  $|\epsilon_r|$  and increase of  $\epsilon_i$ . In addition, we show theoretically that two types of SPs are supported by the

hole arrays in a polaritonic membrane: localized surface polaritons (LSPs) and delocalized SSPs.

Square arrays of round holes were milled by a dual focused ion beam (FIB) system (FEI Strata 235) in a suspended SiC membrane. The starting material for membrane fabrication was a 458 nm thick single-crystalline 3C-SiC film heteroepitaxially grown on the front (polished) side of a 0.5 mm thick Si(100) wafer [20]. The  $0.35 \times 0.35$  mm suspended membrane was produced by anisotropic KOH etching of the Si from the back (unpolished) side [12]. All holes were round in shape (see insets to Fig. 1), with the edge radius of curvature of order 30 nm. The hole diameter and period in different samples varied in the range  $1 \leq D \leq 2\mu\text{m}$  and  $5 \leq L \leq 7\mu\text{m}$ , and a typical perforated area was  $150 \times 150\mu\text{m}$  in size. Inset of the Fig. 1 shows one fabricated sample with  $D = 2\mu\text{m}$  and  $L = 7\mu\text{m}$ . An FTIR microscope (Perkins-Elmer Spectrum GX AutoImage) with spatial domain  $(100\mu\text{m})^2$  has been used to measure the transmission and reflection from the perforated and non-perforated areas in the  $1500 - 700\text{cm}^{-1}$  spectral range. The FTIR microscope utilized Cassegrain optics with the angle of incidence between  $9^\circ - 35^\circ$ . Input IR radiation was polarized by a wire-mesh (ISP Optics) polarizer. To quantify the effect of the holes, transmission and absorption spectra of a non-perforated SiC membrane are subtracted from the corresponding hole array spectra and plotted in Fig. 1 for several values of  $D$  and  $L$ .

Below we focus on the ( $D = 2\mu\text{m}$ ,  $L = 7\mu\text{m}$ ) sample. Although the deeply sub- $\lambda$  holes occupy only  $\eta = 6\%$  of the total sample area, they increase the transmittance through the sample by  $T_h = 20\%$  (from  $T_{\text{film}} = 10\%$  to  $T_{\text{perf}} = 30\%$ ) at  $\lambda_{tr} = 11.95\mu\text{m}$ . This  $\times 3$  transmission increase over the fractional holes' area is quite remarkable; outside of the *reststrahlen* ( $\epsilon(\omega) < 0$ ) region of SiC the increase is much smaller than  $\eta$ . Even more remarkable is the increase of absorption (up by almost 40% from  $< 1\%$  in a non-perforated film) at  $\lambda_{abs} = 11.8\mu\text{m}$ . Other perforated samples ( $L = 5\mu\text{m}$ ,  $D = 1\mu\text{m}$ ) and ( $L = 7\mu\text{m}$ ,  $D = 1\mu\text{m}$ ) were also experimentally studied and gave qualitatively similar results as shown in Fig. 1. The absorption maximum is blue-shifted for smaller holes ( $\lambda_{abs} = 11.57\mu\text{m}$  for the  $L = 7\mu\text{m}$ ,  $D = 1\mu\text{m}$  sample) and for smaller periods ( $\lambda_{abs} = 11.49\mu\text{m}$  for the  $L = 5\mu\text{m}$ ,  $D = 1\mu\text{m}$  sample), in accordance with the theory presented below which explains the anomalies in transmission and absorption as manifestations of surface phonon polariton excitation. This theory paves the way to the engineering of optical properties of polaritonic films using resonant excitation of surface polaritons. More complex three-dimensional materials can

then be built using multi-layer polaritonic films as building blocks.

Because of the sub- $\lambda$  nature of the perforated film, it can be described as an *effective medium* with a frequency-dependent permittivity  $\epsilon_{\text{eff}}(\omega)$  determined by several strongest electrostatic (ES) resonances. Strengths and frequencies of these resonances are numerically computed using two different formalisms: generalized eigenvalue differential equation (GEDE) [22, 23, 24] and the surface integral eigenvalue equation [25, 26]. The former method has been successfully applied to periodic sub- $\lambda$  polaritonic crystals consisting of non-connected polaritonic inclusions [24]. To the best of our knowledge, this is the first generalization of this method to the system with a *continuous* polaritonic phase.

The details of the GEDE approach as applied to periodic nanostructures consisting of two material components (one with a frequency-dependent  $\epsilon(\omega) < 0$  and another with  $\epsilon_d = 1$ ) is described elsewhere [22, 27]. Briefly, the following steps are followed. First, the GEDE  $\vec{\nabla} \cdot [\theta(\vec{x})\vec{\nabla}\phi_i] = s_i\nabla^2\phi_i$  is solved for the real eigenvalue  $s_i$ , where  $\theta(\vec{x}) = 1$  inside the polaritonic material and  $\theta(\vec{x}) = 0$  elsewhere, and  $\phi_i$  is a potential eigenfunction with the dipole symmetry periodic with period  $L$  in the plane of the film. Second, the dipole strengths  $f_i$  proportional to the squared dipole moment of each resonance are calculated [23]. Finally, the ES permittivity  $\epsilon_{\text{eff}}(\omega)$  is found by summing up the contributions of all dipole-active resonances:

$$\epsilon_{\text{eff}}(\omega) = 1 - \frac{f_0}{s(\omega)} - \sum_{i>0} \frac{f_i}{s(\omega) - s_i}, \quad (1)$$

where  $s = [1 - \epsilon(\omega)]^{-1}$  serves as a frequency label. Note the pole at  $s = 0$  (corresponding to  $\epsilon \rightarrow -\infty$ ) in Eq. (1) which emerges due to *continuous* polaritonic phase. “Frequencies”  $s_i$  and strengths  $f_i$  of the dominant dipole resonances computed for the experimentally relevant parameters ( $D = 2\mu\text{m}$ ,  $H = 458\text{nm}$ , and  $L = 7\mu\text{m}$ ) are:  $s_0 = 0$  ( $\epsilon_0 = -\infty$ ) with  $f_0 \approx 0.88$ ,  $s_1 \approx 0.1241$  ( $\epsilon_1 \approx -7.058$ ) with  $f_1 \approx 0.041$ ,  $s_2 \approx 0.1958$  ( $\epsilon_2 \approx -4.107$ ) with  $f_2 \approx 0.0054$ ,  $s_3 \approx 0.255$  ( $\epsilon_3 \approx -2.922$ ) with  $f_3 \approx 0.0036$ , and  $s_4 \approx 0.666$  ( $\epsilon_4 \approx -0.50$ ) with  $f_4 \approx 0.0049$ . Other hole diameters were also studied, and the corresponding  $\epsilon_{1,2}$  are indicated by squares in the inset of Fig. 3. Note that  $\epsilon_{\text{eff}}(\omega)$  is always finite because  $s$  is a complex number due to finite losses in SiC while all  $s_i$  are real.

Experimental results depicted in Fig. 1 can now be interpreted using  $\epsilon_{\text{eff}}(\omega)$ : the normal incidence transmission and reflection coefficients through a slab of thickness  $H$  are given by

$$T = \left| \frac{(1 - r_1^2)e^{ik_0(n-1)H}}{1 - r_1^2e^{2ik_0nH}} \right|^2, \quad R = \left| \frac{r_1(1 - e^{2ik_0nH})}{1 - r_1^2e^{2ik_0nH}} \right|^2,$$

where  $n = \sqrt{\epsilon_{\text{eff}}}$ ,  $k_0 = \omega/c$  and  $r_1 = (1 - n)/(1 + n)$ . The standard polaritonic formula recently verified [12] for suspended SiC membranes was used for  $\epsilon_{\text{SiC}}$ . We have calculated transmittance  $T$  and absorbance  $A = 1 - R - T$  of the perforated film, subtracted the corresponding quantities for the non-perforated film ( $\epsilon_{\text{eff}}$  replaced by  $\epsilon_{\text{SiC}}$ ), and plotted the corresponding differential quantities in Fig. 2. To facilitate the interpretation of the giant transmission and absorption effects, a segment of  $\text{Re}[\epsilon_{\text{eff}}]$ ,  $\text{Im}[\epsilon_{\text{eff}}]$  dependence is plotted in the inset to Fig. 2 near the strongest resonance at  $\lambda_1 = 11.3\mu\text{m}$ , where  $\text{Re}[\epsilon_{\text{SiC}}(\lambda_1)] = \epsilon_1$ .

The absorption spike (dotted line) is due to the peak of  $\text{Im}[\epsilon_{\text{eff}}]$  at  $\lambda = \lambda_1$ . The transmission maximum occurs due to the decrease of the absolute value of  $\text{Re}[\epsilon_{\text{eff}}]$  at  $\lambda = \lambda_{\text{max}}$  shown in the inset (solid line) to Fig. 2. Note that the enhanced transmission predicted from  $\epsilon_{\text{eff}}$  occurs for  $\lambda_{\text{max}} > \lambda_1$  in agreement with experimental observations. Other much smaller absorption and transmission peaks are also predicted. However, experimental accuracy was not sufficient to identify these additional variations of  $T$  and  $A$  in Fig. 1. Because spacing between the holes ( $L = 7\mu\text{m}$ ) was not negligible compared with the wavelength ( $\lambda \sim 11\mu\text{m}$ ), we have carried fully electromagnetic (EM) calculations of  $T$  and  $A$  using the finite-elements frequency domain (FEFD) solver COMSOL. The results displayed in Fig. 2 show qualitative agreement with the  $\epsilon_{\text{eff}}$ -based calculation, with the exception that all transmission and absorption maxima are slightly red-shifted. This red shift is a previously noted [26] phenomenon explained by the EM corrections to the purely ES response of sub- $\lambda$  polaritonic structures.

One manifestation of resonances of  $\epsilon_{\text{eff}}(\omega)$  is an increase of the peak electric field  $E_{\text{max}}$  inside the hole in response to the applied across the structure ac electric field with amplitude  $E_0$ . The ratio of  $E_{\text{max}}/E_0$  is plotted in Fig. 4 as a function of  $\lambda$  for a fixed hole diameter  $D = 2\mu\text{m}$  and variable period  $L$ . Four enhancement spikes corresponding to resonances of  $\epsilon_{\text{eff}}(\omega)$  can be identified for all periods. Frequencies of the three red resonances ( $\lambda > 10.5\mu\text{m}$ ) are located in the  $\text{Re}[\epsilon_{\text{SiC}}] < -1$  band and are all strongly dependent on  $L$ . On the contrary, blue resonance ( $\lambda_{\text{loc}} \approx 10.45\mu\text{m}$ ) belongs to the  $-1 < \text{Re}[\epsilon_{\text{SiC}}] < 0$  range and is period-independent. Another striking difference between the red and blue resonances is that the former are very de-localized, while the latter is strongly localized near the hole (see the two insets to Fig. 4). Identification of the period-independent resonance as the LSP of a single

hole, and of the period-dependent resonances as delocalized waves related to SSPs of the smooth film is one of the main theoretical advances of this Letter.

To validate this identification, we start with reviewing the properties of SPs of a smooth thin negative- $\epsilon$  film surrounded by vacuum. Through symmetry, SPs can be labeled by the parity of the in-plane electric field with respect to the mid-plane, and by a continuous in-plane wavenumber  $k$ . A dispersion relation  $\omega$  vs.  $k$  in the ES limit of  $k \gg \omega/c$  is given implicitly by  $\epsilon_{\pm}(\omega) = -\tanh(kH/2)^{\mp 1}$ , where  $\pm$  refers to even and odd modes, respectively. Note that even (“slow”) modes are located in the  $-\infty < \epsilon < -1$  part of the spectrum, while the odd (“fast”) modes are in the  $-1 < \epsilon < 0$  range. EM corrections to the dispersion relation do not alter this ordering (except for  $k \approx \omega/c$  case that is not relevant to this work). The EM dispersion curve and its ES approximation (expressed as  $\text{Re}[\epsilon_{\text{SiC}}](\omega)$  vs.  $k$ ) for the fast and slow SPs on a smooth SiC film are plotted in Fig. 3.

Because  $k > \omega/c$  for SPs, they cannot be excited by an EM wave incident from vacuum. A *perforated* film, however, acts as a crossed diffraction grating and provides coupling between normally incident radiation (with almost uniform electric field  $\vec{E}_0 = E_0 \vec{e}_x$ ) and surface modes of the film with the in-plane wavenumbers  $k_{(m,n)} = \left| \frac{2\pi}{L}(m\hat{x} + n\hat{y}) \right| \equiv \frac{2\pi}{L} \sqrt{m^2 + n^2}$  [28]. Resonances of  $\epsilon_{\text{eff}}(\omega)$  can be understood as the result of strong coupling of  $\vec{E}_0$  to *slow* surface polaritons (SSP( $m, n$ )) [28]. This interpretation is verified by extrapolating the diameter-dependent resonant  $\epsilon$  for the two low-frequency eigenmodes to  $D = 0$  shown in the inset to Fig. 3. It is apparent from Fig. 3 that these two resonances correspond to excitation of SSP(0, 1) and SSP(1, 1) of the smooth film. Another conclusion that can be drawn from Fig. 3 is that EM effects shift the frequencies of SPs towards red. This explains the red shift of transmission and absorption spikes in EM simulations from their positions in ES model.

No identification with one of the smooth film SSPs can be made for the LSP resonance at  $\lambda = 10.45 \mu\text{m}$ . In fact, this highly localized near the hole perimeter surface wave resonance can be thought of as an even-parity “defect state” created by the presence of a single hole in a negative- $\epsilon$  film. Because the frequency range for which  $-1 < \epsilon(\omega) < 0$  is a stop-band for even-parity propagating SPs, the even-parity LSP can exist in this, and only this frequency range. Because of the localized nature of the LSP, its frequency is insensitive to the proximity of other holes (i. e. to the period  $L$ ) but is sensitive to the aspect ratio of the hole and even to the radius of curvature of hole edge.

In conclusion, we have experimentally demonstrated giant absorption and transmission

through optically thin SiC membranes perforated by a rectangular array of round holes. These effects are theoretically explained by introducing the effective permittivity of a perforated membrane with a complex frequency dependence due to resonant coupling to almost-ES surface phonon polaritons. Two types of phonon polariton resonances are theoretically uncovered: (i) delocalized modes related to the SSPs of a smooth film, and (ii) a localized surface polariton (LSP) of a single hole that exists in the spectral range complementary to that of SSPs.

This work is supported by the ARO MURI W911NF-04-01-0203 and the DARPA contract HR0011-05-C-0068. We gratefully acknowledge Drs. A. Aliev and A. A. Zakhidov for their assistance with FTIR microscopy and Dr. C. Zorman for growing SiC films and useful discussions.

- 
- [1] E.Ozbay, *Science* **31**, 189 (2006).
  - [2] W. L. Barnes, A. Dereux, and T. W. Ebbesen, *Nature* **424**, 824 (2003).
  - [3] R. Hillenbrandt, T. Taubner, and F. Keilmann, *Nature* **418**, 159 (2002).
  - [4] P.Berini, *Phys. Rev.B* **63**, 125417 (2001).
  - [5] R.Zia, M.D.Selker, P.B.Catrysse, and M.L.Brongersma, *JOSA A* **21**, 2442 (2004).
  - [6] A. Huber, N. Ocelic, D. Kazantsev, and R. Hillenbrandt, *Appl. Phys. Lett.* **87**, 081103 (2005).
  - [7] G. Shvets, *Phys. Rev. B.* **338**, 035109 (2003).
  - [8] H. Shin and S. Fan, *Phys. Rev. Lett.* **96**, 073907 (2006).
  - [9] A. Alu and N. Engheta, *JOSA B* **23**, 571 (2006).
  - [10] N. Fang, H. Lee, C. Sun, and X. Zhang, *Science* **308**, 534 (2005).
  - [11] D. O. S. Melville and R. J. Blaikie, *Optics Express* **13**, 2127 (2005).
  - [12] D. Korobkin, Y. Urzhumov, and G. Shvets, *JOSA B* **23**, 468 (2005).
  - [13] S. I. Bozhevolnyi, V. S. Volkov, E. Devaux, J.-Y. Laluet, and T. W. Ebbesen, *Nature* **440**, 508 (2006).
  - [14] F. Le, N. Z. Lwin, J. M. Steele, M. Kall, N. J. Halas, and P. Nordlander, *Nano Letters* **5**, 2009 (2005).
  - [15] T. Ebbesen, *Nature* **391**, 667 (1998).
  - [16] J. Prikulis, P. Hanarp, L. Olofsson, D. Sutherland, and M. Kall, *Nano Letters* **4**, 1003 (2004).

- [17] Q. Cao and P. Lalanne, *Phys. Rev. Lett* **88**, 057403 (2002).
- [18] H. Lezec and T. Thio, *Opt. Exp.* **12**, 3629 (2004).
- [19] J. B. Pendry, L. Martin-Moreno, and F. J. Garcia-Vidal, *Science* **305**, 847 (2004).
- [20] C. Zorman, *J. Appl. Phys.* **78**, 5136 (1995).
- [21] J.-J. Greffet, R. Carminati, K. Joulain, J.-P. Mulet, S. Mainguy, and Y. Chen, *Nature* **416**, 61 (2002).
- [22] D. Bergman and D. Stroud, *Solid State Phys.* **46**, 147 (1992).
- [23] M. I. Stockman, S. V. Faleev, and D. J. Bergman, *Phys. Rev. Lett.* **87**, 167401 (2001).
- [24] G. Shvets and Y. Urzhumov, *Phys. Rev. Lett.* **93**, 243902 (2004).
- [25] D. R. Fredkin and I. D. Mayergoyz, *Phys. Rev. Lett.* **91**, 253902 (2003).
- [26] I. D. Mayergoyz, D. R. Fredkin, and Z. Zhang, *Phys. Rev. B* **72**, 155412 (2005).
- [27] G. Shvets and Y. A. Urzhumov, *J. Opt. A: Pure Appl. Opt.* **7**, S23 (2005).
- [28] A. Degiron, H. Lezec, N. Yamamoto, and T. Ebbesen, *Opt. Comm.* **239**, 61 (2004).



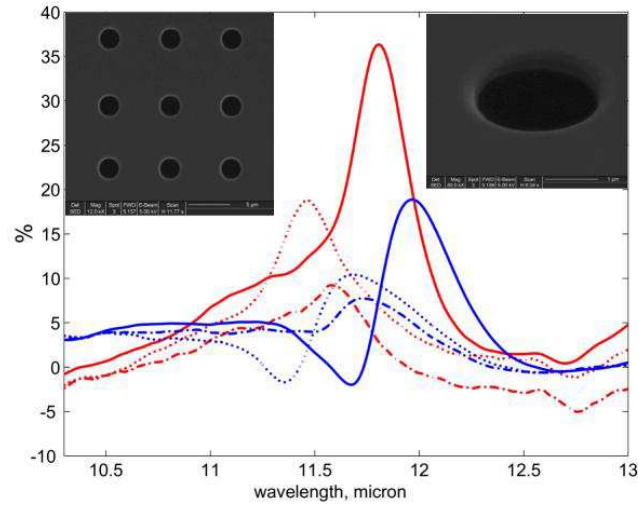


FIG. 1: (Color online) Extra transmission (blue) and absorption (red) of square arrays of circular holes in a 458nm thick SiC film, relative to non-perforated film. Solid:  $L = 7\mu\text{m}$ ,  $D = 2\mu\text{m}$ ; dash-dotted:  $L = 7\mu\text{m}$ ,  $D = 1\mu\text{m}$ ; dotted:  $L = 5\mu\text{m}$ ,  $D = 1\mu\text{m}$ . Left inset: SEM image of the  $L = 7\mu\text{m}$ ,  $D = 2\mu\text{m}$  sample. Right inset: SEM image of a  $D = 2\mu\text{m}$  hole (at  $52^\circ$  from normal).

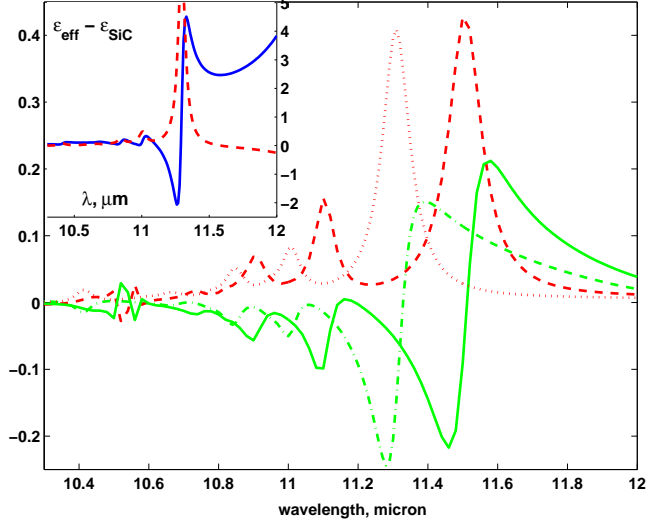


FIG. 2: (Color online) Theoretical extra transmission (green solid and dash-dotted curves) and absorption (red dashed and dotted curves) of a  $7\mu\text{m}$  array of  $2\mu\text{m}$  holes in  $458\text{ nm}$  film of SiC. Solid and dashed curves: FEFD simulation of EM wave scattering; dash-dotted and dotted: theoretic estimate based on ES  $\epsilon_{\text{eff}}$ , which is plotted on the inset.

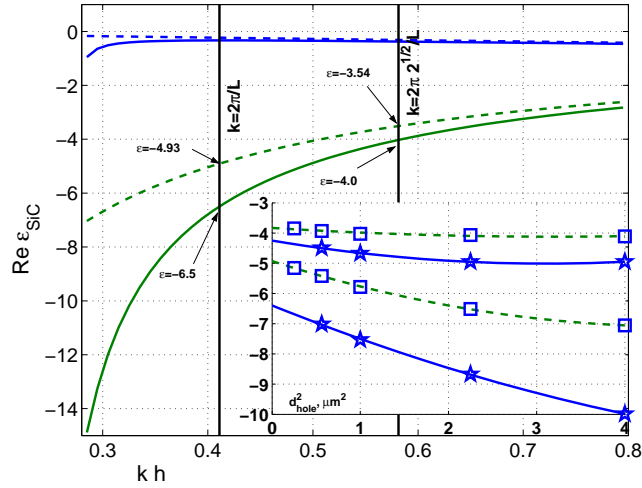


FIG. 3: (Color online) Dispersion relation of the even (green, lower curves) and odd (blue, upper curves) surface polaritons on a SiC film with thickness  $H = 458\text{ nm}$ . Solid lines: exact dispersion relation in the form of  $\text{Re}[\epsilon_{\text{SiC}}(\omega)]$  vs.  $k$ , dashed lines: ES approximation. Two vertical lines:  $k = 2\pi/L$  and  $k = 2\sqrt{2}\pi/L$  for  $L = 7\mu\text{m}$ . Inset: position of delocalized resonances SSP(1,0) and SSP(1,1) as a function of hole diameter  $D$  (squares on dashed line - ES eigenvalue simulations; stars on solid line - absorption peak positions in EM FEFD simulations).

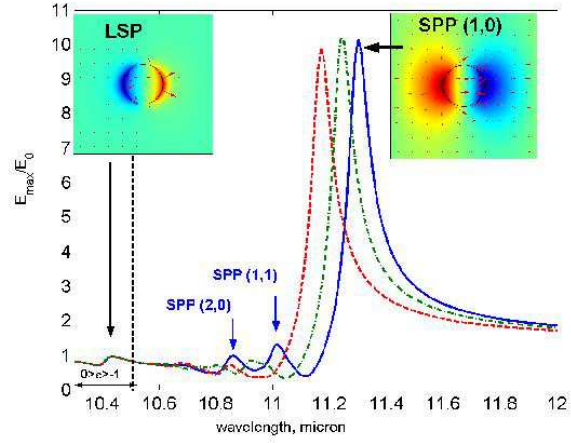


FIG. 4: (Color online) Electric field enhancement in the symmetry plane of a SiC film perforated with a  $L = 7\mu\text{m}$ -period square array of  $D = 2\mu\text{m}$  round holes. Insets: ES potential profile at the resonances: (left) LSP resonance, and (right) SPP(1,0) resonance.